

Phosphorylation of a membrane curvature-sensing motif switches function of the HOPS subunit Vps41 in membrane tethering

Margarita Cabrera,¹ Lars Langemeyer,¹ Muriel Mari,³ Ralf Rethmeier,¹ Ioan Orban,² Angela Perz,¹ Cornelia Bröcker,¹ Janice Griffith,³ Daniel Klose,² Heinz-Jürgen Steinhoff,² Fulvio Reggiori,³ Siegfried Engelbrecht-Vandré,¹ and Christian Ungermann¹

¹Department of Biology/Chemistry, Biochemistry Section, and ²Department of Physics, Experimental Physics Section, University of Osnabrück, 49076 Osnabrück, Germany
³Department of Cell Biology, Institute of Biomembranes, University Medical Centre Utrecht, 3584 CX Utrecht, Netherlands

Tethering factors are organelle-specific multisubunit protein complexes that identify, along with Rab guanosine triphosphatases, transport vesicles and trigger their SNARE-mediated fusion of specific transport vesicles with the target membranes. Little is known about how tethering factors discriminate between different trafficking pathways, which may converge at the same organelle. In this paper, we describe a phosphorylation-based switch mechanism, which allows the homotypic vacuole fusion protein sorting effector subunit Vps41 to operate in two distinct fusion events, namely endosome–vacuole and AP-3 vesicle–vacuole fusion. Vps41 contains an amphipathic lipid-packing sensor (ALPS) motif, which recognizes

highly curved membranes. At endosomes, this motif is inserted into the lipid bilayer and masks the binding motif for the δ subunit of the AP-3 complex, Apl5, without affecting the Vps41 function in endosome–vacuole fusion. At the much less curved vacuole, the ALPS motif becomes available for phosphorylation by the resident casein kinase Yck3. As a result, the Apl5-binding site is exposed and allows AP-3 vesicles to bind to Vps41, followed by specific fusion with the vacuolar membrane. This multifunctional tethering factor thus discriminates between trafficking routes by switching from a curvature-sensing to a coat recognition mode upon phosphorylation.

Introduction

Several distinct protein complexes orchestrate the fusion of lipid bilayers along the secretory and endocytic pathways in eukaryotic cells. The initial recognition of membranes requires the conversion of a specific Rab GTPase to its GTP form, followed by the recruitment of effector proteins, including tethering complexes and phosphoinositide kinases. The final mixing of lipid bilayers is catalyzed by the assembly of membrane-embedded SNARE proteins from both membranes. Tethering complexes consist of several subunits with distinct activities to coordinate this reaction cascade: they are large enough to bridge

membranes and bind Rab-GTP and may bind SNAREs to guide and control the fusion reaction. This includes the exocyst complex of the plasma membrane (TerBush et al., 1996), the conserved oligomeric Golgi complex at the Golgi (Ungar et al., 2002), the Dsl complex at the ER, or the Golgi-associated retrograde protein complex, which operates between endosome and Golgi (Conibear et al., 2003). We focus on the homotypic vacuole fusion protein sorting (HOPS) complex, which binds to the Rab7 GTPase Ypt7 to mediate fusion at the vacuole (Seals et al., 2000). This complex consists of six subunits, four of which (Vps11, Vps16, Vps18, and Vps33) are found also in the homologous endosomal class C core vacuole/endosome tethering complex (Peplowska et al., 2007). In addition, the HOPS complex

M. Cabrera and L. Langemeyer contributed equally to this paper.

Correspondence to Siegfried Engelbrecht-Vandré: engel@uos.de; or Christian Ungermann: cu@uos.de

Abbreviations used in this paper: ALP, amphipathic lipid packing; ALPS, ALP sensor; CPY, carboxypeptidase Y; EPR, electron paramagnetic resonance; GMAP, Golgi-associated microtubule protein; HOPS, homotypic vacuole fusion protein sorting; MBP, maltose-binding protein; MVB, multivesicular body; wt, wild type; YPD, yeast peptone D-glucose.

© 2010 Cabrera et al. This article is distributed under the terms of an Attribution–Noncommercial–Share Alike–No Mirror Sites license for the first six months after the publication date [see <http://www.rupress.org/terms>]. After six months it is available under a Creative Commons License [Attribution–Noncommercial–Share Alike 3.0 Unported license, as described at <http://creativecommons.org/licenses/by-nc-sa/3.0/>].

contains two Rab-binding proteins: Vps39/Vam6 binds Ypt7 independently of its nucleotide load and most likely apart from the HOPS complex (Ostrowicz et al., 2010), whereas Vps41/Vam2 is the Rab effector subunit of HOPS (Brett et al., 2008). Recent data showed that Ypt7 also localizes to late endosomes (kleine Balderhaar et al., 2010), where it is activated via the Mon1–Ccz1 guanine nucleotide exchange factor complex (Nordmann et al., 2010).

Both the carboxypeptidase Y (CPY) pathway, which passes through the endosome, and the direct AP-3 pathway (TGN to vacuole) depend on the same fusion machinery at the vacuole, composed of the HOPS complex, Ypt7, and vacuolar SNAREs. The AP-3 pathway is conserved across species and directs cargo from early endosomes to late endosomes or lysosomes in mammalian cells (Dell'Angelica, 2009). In yeast, AP-3 vesicles fuse directly with the vacuole but not late endosomes (Cowles et al., 1997). Protein sorting via this pathway depends on the AP-3 complex, which is composed of δ , β 3, μ 3, and σ 3 subunits (Cowles et al., 1997). Interestingly, Vps41 of the HOPS complex has been linked to the AP-3 pathway because both isolated and HOPS-integrated Vps41 binds the δ subunit of the AP-3 complex, Apl5 (Rehling et al., 1999; Darsow et al., 2001). Consequently, Vps41 may be involved in recognizing AP-3 vesicles at the vacuole (Angers and Merz, 2009).

Previously, we have identified the casein kinase Yck3 as a regulator of Vps41 (LaGrassa and Ungermann, 2005). Yck3 is targeted directly to vacuoles via the AP-3 pathway, thus bypassing the endosomes (Sun et al., 2004). In cells lacking Yck3, Vps41 is concentrated at contact sites between endosomes and vacuoles. It remains functional in endosome–vacuole fusion (LaGrassa and Ungermann, 2005; Cabrera et al., 2009) but is defective in the AP-3 pathway (Anand et al., 2009; Cabrera et al., 2009). Identification of the phosphorylation site within Vps41 has revealed that this protein contains two regions that promote its association with membranes, one binding to Ypt7 and another one controlled by Yck3-mediated phosphorylation (Cabrera et al., 2009).

Here, we identify the mechanism that allows Vps41 to discriminate between two distinct transport pathways targeted to the same organelle. At late endosomes, Vps41 binds to both Ypt7-GTP and membranes via an amphipathic lipid-packing (ALP) sensor (ALPS) motif (Bigay et al., 2005; Drin et al., 2007) located within its N-terminal domain. The embedding of the ALPS motif in the membrane masks a proximal AP-3-binding site in Vps41. At the vacuole, in contrast, the ALPS motif is released from the membrane and phosphorylated by the vacuolar casein kinase Yck3, thus exposing the AP-3-binding site in Vps41. Consequently, AP-3 vesicles can only fuse with vacuoles but not with endosomes. This explains how one tethering factor can determine fusion specificity at different organelles.

Results

Vps41 is detected on late endosomes

The AP-3 pathway in yeast is important for the selective delivery of the syntaxin Vam3 and the R-SNARE Nyv1 to the lysosome-like vacuole, thus providing identity to this organelle.

Mutations in the molecular machinery involved in this pathway have been linked to multiple diseases in mammalian cells (Dell'Angelica, 2009). In yeast, the AP-3 pathway delivers proteins directly to the vacuole, bypassing the endosomes, and it depends on the same fusion machinery that also mediates endosome–vacuole fusion. The mechanism responsible for this fusion selectivity is not yet known. Transport across the AP-3 pathway can be monitored with the help of a highly sensitive GFP-tagged reporter protein termed GNS. This construct is composed of the N-terminal cytoplasmic part of the vacuolar SNARE Nyv1 fused with the transmembrane region of the SNARE Snc1 involved in exocytosis (Reggiori et al., 2000). GNS is targeted directly from the Golgi to the vacuole via the AP-3 pathway because the cytoplasmic domain of Nyv1 possesses a dileucine motif necessary to enter this transport route (Fig. 1 A). If the AP-3 pathway is defective, GNS is targeted instead to the plasma membrane and partially to the vacuole via the CPY pathway (Fig. 1 A). Thus, plasma membrane staining of GNS readily identifies defects in AP-3 transport, as observed for deletion in the AP-3 subunit Apl5, which eliminates AP-3 vesicle generation (Fig. 1 B). Deletion of the casein kinase Yck3, which phosphorylates the HOPS subunit Vps41, causes a partial AP-3-sorting defect, though the reason for this has remained unclear (Fig. 1 B; Anand et al., 2009; Cabrera et al., 2009). GNS missorting can be further enhanced by a *PEP12* deletion, which blocks the CPY pathway, but is not affected in the endocytosis mutant end4-1 (Fig. 1 B). Plasma membrane staining of GNS is, therefore, taken as a general tool to monitor AP-3 defects throughout this study because other AP-3 cargo, such as ALP/Pho8 and Nyv1 (Fig. S1; Reggiori et al., 2000), only revealed a complete block of the AP-3 pathway.

We previously identified a phosphorylation site within the N-terminal part of Vps41 (residues S367, S368, S371, and S372). A nonphosphorylatable Vps41 S-A mutant reproduces the *yck3 Δ* phenotype by blocking AP-3 sorting, whereas a phosphomimetic S-D mutant remains functional (Cabrera et al., 2009). Moreover, in *yck3 Δ* cells, Vps41 together with Vps39 accumulates at endosome–vacuole contact sites that can be stained transiently with the endocytosed lipophilic dye FM4-64 (Fig. 1 C). These sites persisted in *apl5 Δ* cells, indicating their independence of AP-3 function (Fig. S2).

To determine the ultrastructure of these sites, we used a recently established protocol to follow endocytosed Nanogold particles by electron microscopy in the *yck3 Δ* strain (Griffith and Reggiori, 2009). Using the same conditions as used for FM4-64 uptake (Fig. 1 C), we observed Nanogold particles in multivesicular bodies (MVBs) close to the vacuole surface (Fig. 1 D, a and b). Often, MVBs were found in small clusters. Similar accumulations of Nanogold particles inside the MVBs have been observed in cells lacking the vacuolar SNARE Vam3 (Griffith and Reggiori, 2009). Therefore, we wondered whether these MVBs also carried Vps41 and used antibodies against the N-terminal GFP tag to examine GFP-Vps41 localization. Strikingly, some Vps41-positive immunogold particles were detected not only at the limiting membrane of the vacuole but also on the surface of

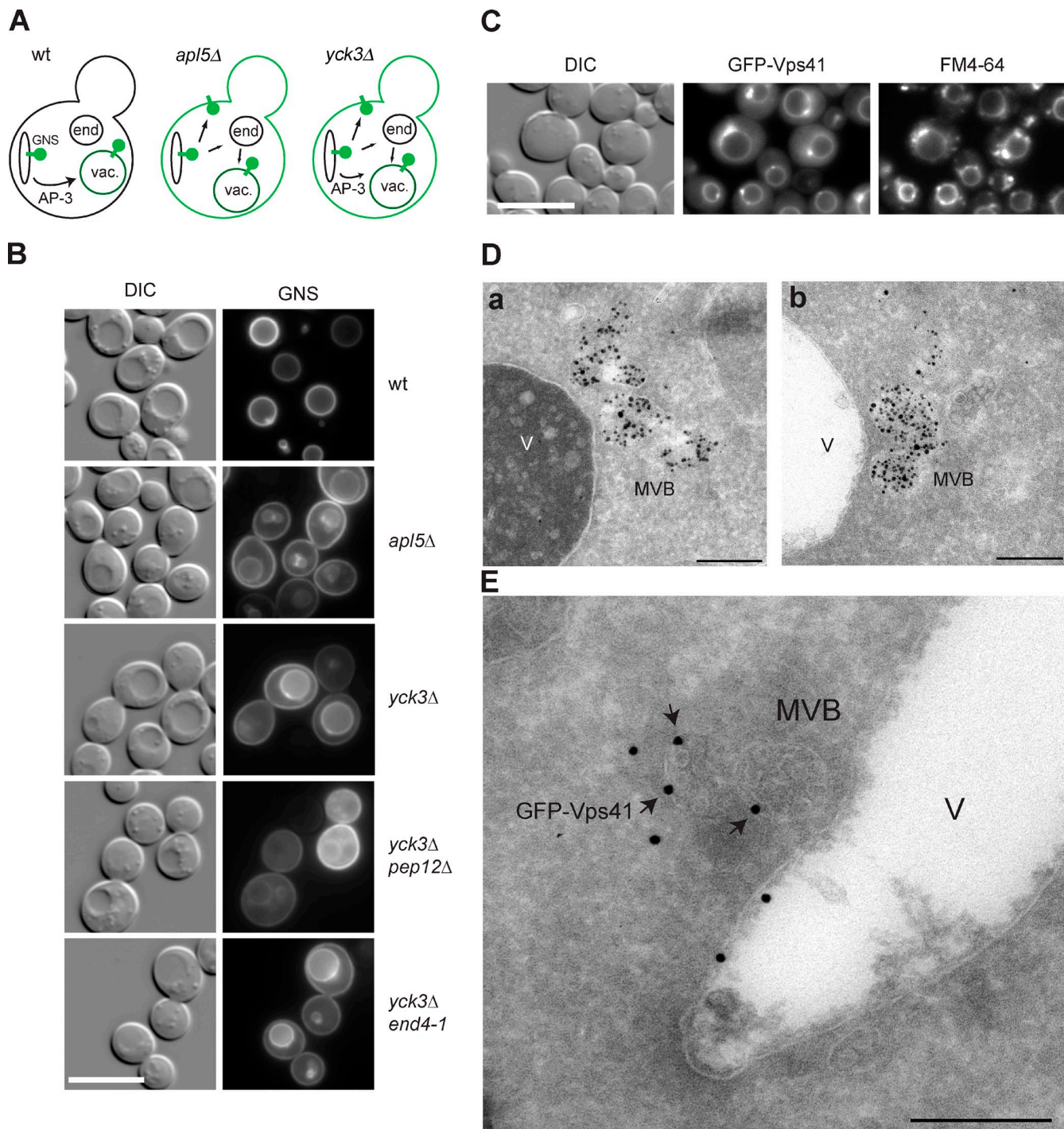


Figure 1. **Ultrastructural localization of Vps41 to late endosomes.** (A) Sorting of the GNS fusion protein via the AP-3 pathway. The protein GNS (GFP-tagged Nyv1-Snc1TMD construct) as well as membranes stained by GNS are shown in green. In wild-type (wt) cells, GNS directly reaches the vacuole, whereas it is sorted via the plasma membrane if the AP-3 pathway is defective. vac., vacuole. (B) Analysis of the AP-3 pathway. GNS is missorted to the plasma membrane in cells lacking Vps41 phosphorylation. The GNS-sorting defect of *yck3Δ* cells was enhanced in *pep12Δ* but not in the *end4-1* mutant (RH1597). (C) Colocalization of GFP-Vps41 and FM4-64. FM4-64 uptake was monitored in the *yck3Δ* strain overexpressing GFP-tagged Vps41. Cells were incubated with the fluorescent dye FM4-64 on ice for 15 min and, after washing, were transferred at 30°C for 20 min. (B and C) Bars, 10 μm. (D) Nanogold labeling of endosomes (a and b). Using the same strain and conditions as used for FM4-64 uptake (B), we observed Nanogold particles in multiple multivesicular bodies (MVBs) close to the vacuole. Bars, 200 nm. (E) Immunoelectron microscopy localization of GFP-Vps41 in the absence of Yck3. Vps41 was visualized using antibodies against GFP. Vps41-positive immunogold particles were detected not only at the limiting membrane of the vacuole but also on MVB surfaces. DIC, differential interference contrast. V, vacuole. Bar, 200 nm.

MVBs (Fig. 1 E). The labeling was weak but specific, suggesting a partial occlusion of the antigen. Obviously, Vps41 accumulates at MVBs in the absence of Yck3. Together, these

observations show that the localization of Vps41 to endosomes and its functionality in the AP-3 pathway are controlled by its phosphorylation state.

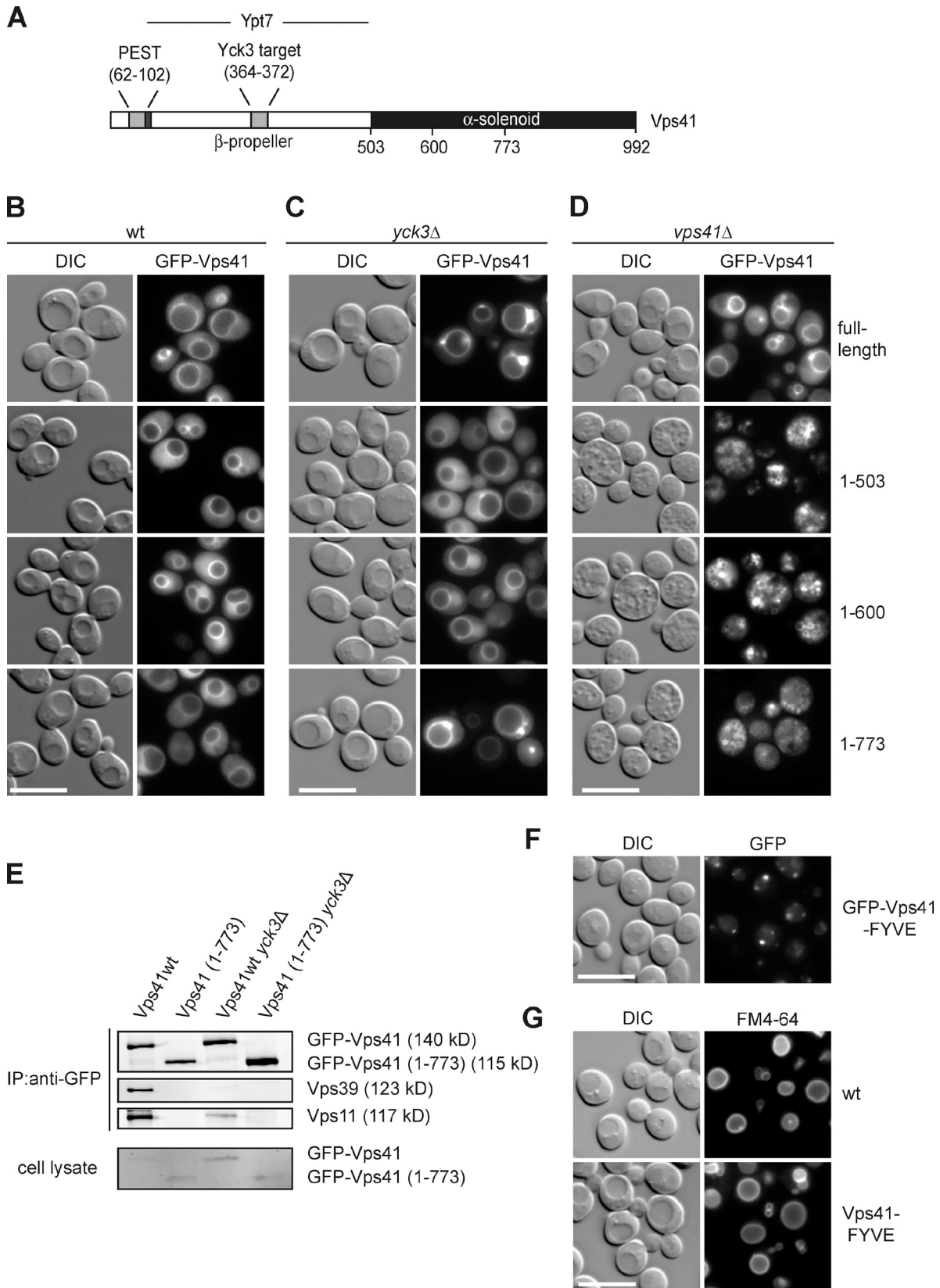


Figure 2. **Identification of the Vps41 vacuole-targeting domain.** (A) Diagram of Vps41 domain organization and interactions. (B) Vacuole targeting of Vps41. wt strains expressing the indicated fragments of GFP-tagged Vps41 were examined by fluorescence microscopy. (C) Vps41 distribution in the absence of Vps41. Full-length protein and C-terminal truncations of Vps41 were visualized in the *yck3Δ* strain as before. (D) The vacuole morphology in the *vps41Δ* strain expressing full-length protein or C-terminal truncations of Vps41 was analyzed using fluorescence microscopy. (E) The C-terminally truncated Vps41(1-773) is not incorporated into the HOPS complex. GFP antibodies coupled to protein A-Sepharose were used to precipitate GFP-tagged full-length and truncated (1-773 fragment) Vps41 from cell lysates. The top three panels show the anti-GFP immunoprecipitates that were probed with

Vps41 targeting to endosomes is independent of the HOPS complex assembly

Next, we asked whether we could identify a minimal domain of Vps41 that would localize the protein to late endosomes in a Yck3-dependent manner. Fig. 2 A summarizes the known structural and functional assignments for Vps41. We generated C-terminal deletion constructs, all N-terminally tagged with GFP, and localized them in both wild-type (wt) and *yck3Δ* cells (Fig. 2, B and C). The N-terminal domain (residues 1–503), which also contains a binding site for Ypt7 (Brett et al., 2008; Ostrowicz et al., 2010), is sufficient for targeting Vps41 to the vacuole (Fig. 2 B). On the other hand, only the truncated protein Vps41(1–773) responded to the *YCK3* deletion like the wt protein (Fig. 2 C). Despite its endosomal localization in *yck3Δ* cells, the Vps41(1–773) construct was not integrated into the HOPS complex (Fig. 2 E), and it did not complement *vps41Δ* cells (Fig. 2 D). These data suggest that endosomal targeting of Vps41 depends on at least two domains rather than just its incorporation into the HOPS holocomplex.

We then asked whether Vps41 would remain functional in endosome–vacuole fusion if we would artificially target it to late endosomes. We therefore fused Vps41 to the EEA1 FYVE domain, which binds phosphoinositide-3-phosphate (Stenmark et al., 1996). The FYVE-tagged Vps41 protein strongly localized to the endosome, with some residual staining on the vacuole membrane (Fig. 2 F). Surprisingly, the endosomal Vps41-FYVE did not result in vacuole fragmentation (Fig. 2 G), indicating that it is incorporated into the HOPS complex and supports endosome–vacuole fusion. Our data are in agreement with the idea that Vps41 is initially targeted to late endosomes and is then transferred to the vacuole.

Identification of the Vps41 ALPS motif

How does Vps41 associate with late endosomes? A recent bioinformatic survey predicted an ALPS within the N-terminal domain of Vps41 (Drin et al., 2007). The ALPS motif constitutes a particular α helix suitable for binding to highly curved membranes (Fig. 3 A; Bigay et al., 2005). This motif (residues 359–376) overlaps with the Yck3 phosphorylation sites (residues S367, S368, S371, and S372) identified previously (Cabrera et al., 2009). We therefore generated Vps41 ALPS mutants by either inserting a negative charge into the hydrophobic face (L366D) or deleting an entire segment of the putative helix (residues 366–377, termed Δ ALPS). Either mutant resembled the phosphomimetic version of Vps41 S-D; e.g., both mutant proteins poorly localized to vacuoles, and cells expressing these mutants displayed multilobed vacuoles (Fig. 3, B and D; Cabrera et al., 2009).

As mentioned in the Introduction, Vps41 is recruited to the membranes by interacting with the Rab GTPase Ypt7 in its

GTP form (Brett et al., 2008; Ostrowicz et al., 2010). We observed previously that GFP tagging of Ypt7 has no obvious effect on the localization of Vps41 and vacuole morphology of wt cells. However, in the Vps41 S-D mutant, which is already poorly localized to vacuoles, GFP tagging of Ypt7 leads to vacuole fragmentation (Cabrera et al., 2009). We concluded from these observations that the GFP tag interferes with the binding of Ypt7 to Vps41. If the ALPS motif is indeed an additional membrane-targeting motif, one would expect a similar effect upon GFP tagging of Ypt7 in the ALPS mutants. This was indeed the case (Fig. 3 C), suggesting that interference with helix formation affects Vps41 function. To test whether isolated Vps41 by itself binds to membranes, we purified full-length N-terminally His-tagged Vps41 from bacteria and subjected it to flotation with liposomes of defined curvature using an established protocol (Bigay et al., 2005). Strikingly, full-length Vps41 floated efficiently with small liposomes in the top fraction of the gradient (Figs. 3 E and S3 A). The N-terminal domain of Vps41 (residues 1–484) behaved similarly to the wt protein in this respect (Figs. 3 F and S3 B). Flotation of Vps41 was completely blocked, however, by either the L366D or Δ ALPS mutations (Figs. 3 F and S3 B), thus indicating that Vps41 contains an ALPS motif in this region, which is required for efficient binding to small vesicles.

To clarify whether this motif folds into an α helix, we turned to electron paramagnetic resonance (EPR), which allows inter-residue distance determination. We fused residues 336–403 of Vps41 to the maltose-binding protein (MBP) and included Cys substitutions at residues 366 and 373 of the hydrophobic face, followed by cross-linking to the spin label methanethiosulfonate (Fig. 3 G). We determined the distance of the two spin labels by EPR at 1.1 nm, equivalent to the distance of two helical turns of an α helix (Fig. 3 K). Using molecular dynamics simulation, we modeled all possible orientations of the spin labels and confirmed the α -helical structure of the ALPS motif (Fig. 3, H–K). Vps41 thus contains a sequence that can form an amphipathic α helix, which is required for its association to membranes and correct localization.

Targeting of Vps41 by an alternative ALPS motif

To test whether the ALPS motif dictates Vps41 membrane targeting, we replaced it by the ALPS motif of Golgi-associated microtubule protein-210 (GMAP-210) (Fig. 4 A; Drin et al., 2007, 2008). This mutant was targeted to vacuoles, complemented the vacuole fragmentation phenotype of the *vps41Δ* cells, and was insensitive to tagging of Ypt7 with GFP (Fig. 4, B and C). In contrast to the wt protein, Vps41-GMAP was not phosphorylated by Yck3, and its localization was not affected by deleting this kinase (Fig. 4, C and D). The Yck3-mediated size shift of the phosphorylated wt Vps41 is comparable with

anti-GFP, anti-Vps39, and anti-Vps11 antibodies, whereas the bottom panel shows the immunoblot of total cell lysates. (F and G) Targeting of Vps41 to endosomes via the EEA1 FYVE domain. (F) Cells expressing GFP-Vps41 and GFP-Vps41-FYVE under the alcohol dehydrogenase promoter were grown in yeast peptone + glycerol and analyzed by fluorescence microscopy. (G) FM4-64 staining of vacuoles from wt and Vps41-FYVE strains. DIC, differential interference contrast. Bars, 10 μ m.

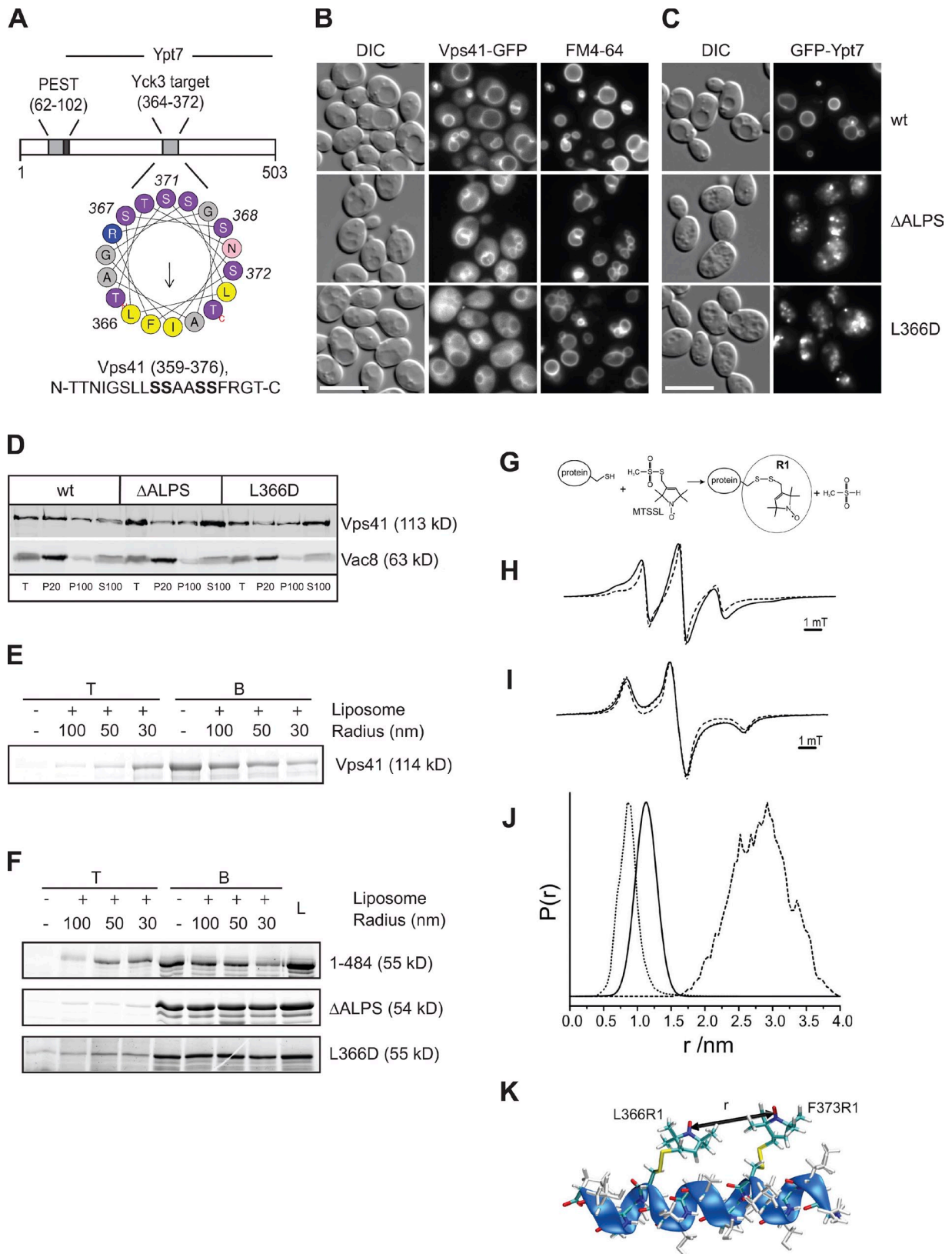


Figure 3. **Vps41 contains an ALPS motif.** (A) Helical wheel representation of residues 359–376 of Vps41 using Heliquest (Gautier et al., 2008). Yellow, hydrophobic residues; purple, serine and threonine; blue, basic; pink, asparagine; and gray, other residues. The phosphorylated residues are indicated in bold in the sequence. The arrow corresponds to the hydrophobic moment. (B) Mutations in the ALPS motif of Vps41 influence Vps41 localization and vacuole morphology. Strains expressing the indicated GFP-Vps41 mutant proteins were labeled with the vacuole marker FM4-64 and analyzed by fluorescence microscopy. (C) GFP tagging of Ypt7 enhances the vacuole fragmentation in cells expressing the Vps41 ALPS point mutants. Strains analyzed in B expressing N-terminal GFP-tagged Ypt7 were visualized by fluorescence microscopy. Bars, 10 μ m. (D) Subcellular fractionation of wt and Vps41 point

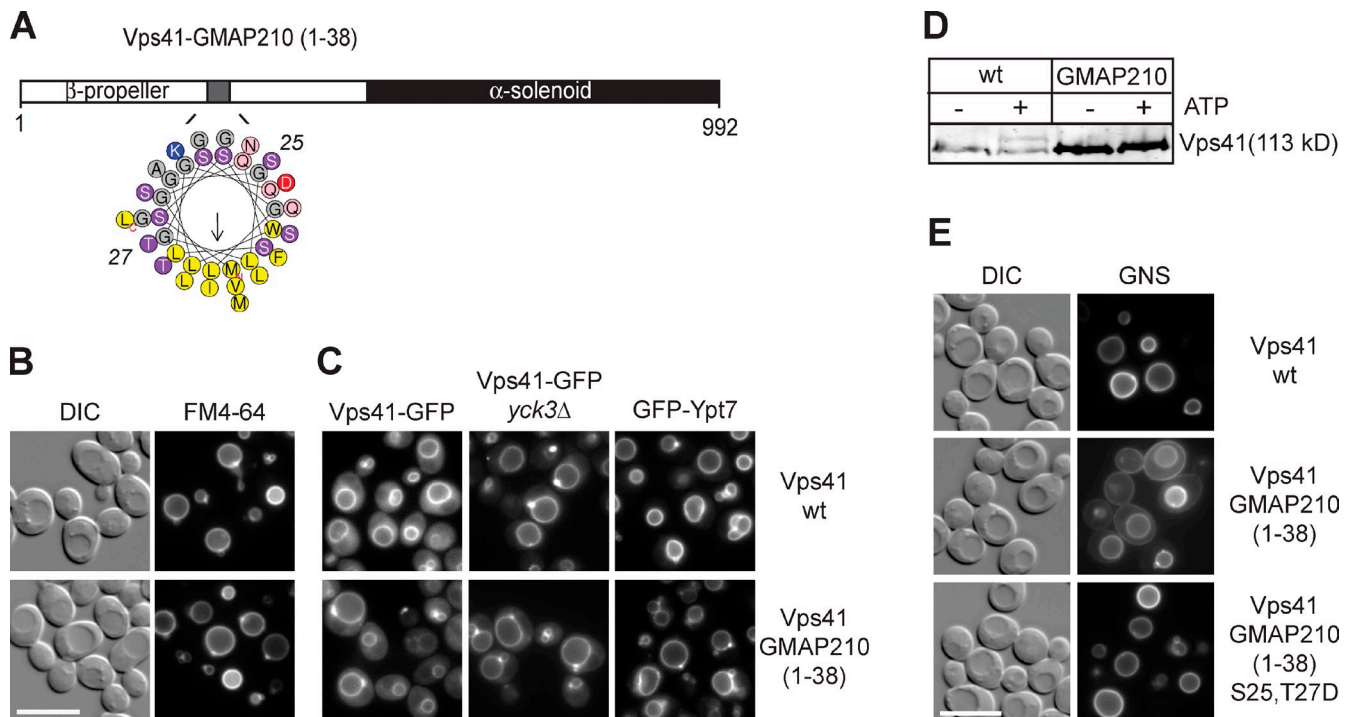


Figure 4. Targeting of Vps41 by an alternative ALPS motif. (A) Helical wheel representation of the 1–38 sequence of GMAP-210 corresponding to the ALPS motif. Yellow, hydrophobic residues; purple, serine and threonine; blue, basic; pink, asparagine; red, acid residue; and gray, other residues. The arrow corresponds to the hydrophobic moment. (B and C) Effect of ALPS motif substitution on Vps41 functions. Vacuole morphology (B), Vps41, and Ypt7 (C) localization were monitored in wild type (wt) or *yck3Δ* strains expressing Vps41 wt or Vps41 carrying the N-terminal 38 residues of GMAP-210 protein. For C, differential interference contrast (DIC) pictures are not depicted. (D) ALPS motif phosphorylation. Membranes obtained from wt- and Vps41-GMAP-210-expressing strains were incubated without and with ATP, and the electrophoretic mobility shift of Vps41 was analyzed by immunoblotting using anti-Vps41 antibodies. (E) Vps41 requires ALPS phosphorylation to function in the AP-3 pathway. The vacuole sorting of GNS was examined in the indicated strains. Bars, 10 μ m.

observations in previous studies (LaGrassa and Ungermann, 2005; Brett and Merz, 2008; Brett et al., 2008; Cabrera et al., 2009; Hickey et al., 2009). Despite its association with the vacuole, the Vps41-GMAP fusion protein was defective in the AP-3 transport pathway because the GNS reporter appeared at the plasma membrane (Fig. 4 E). This sorting defect could be rescued by the phosphomimetic mutations S25 and T27D within the ALPS motif of GMAP-210 (Fig. 4 E). We conclude that Vps41 can only function efficiently in the AP-3 pathway if its ALPS motif can be phosphorylated.

Identification of the Apl5-binding site in Vps41

So far, these data indicated (a) that the ALPS motif of Vps41 is required for its efficient localization; (b) that this motif contains the Yck3 phosphorylation sites; and (c) that loss of Vps41 phosphorylation blocks AP-3 cargo sorting. How then is Vps41 connected to the AP-3 pathway? It has previously been shown that the N-terminal region of Vps41 (residues 99–230) interacts with the AP-3 subunit Apl5 (Darsow et al., 2001; Angers and Merz, 2009). To identify the precise Apl5-binding site,

mutants. Cells expressing C-terminally GFP-tagged Vps41 wt or point mutant forms were lysed, and membranes were separated into pellet (P20) and supernatant fractions at 20,000 *g* for 15 min at 4°C. After centrifugation of the resulting supernatant at 100,000 *g* for 1 h at 4°C, the pellet (P100) and supernatant (S100) were collected and subjected to immunoblot analysis using anti-Vps41 and anti-Vac8 antibodies. T = 50% of total protein used for each separation. (E and F) Flotation assay. Full-length Vps41 (E) or C-terminal truncations (1–484; F) carrying the indicated mutations were incubated with liposomes of decreasing size or buffer (Bigay et al., 2005). After centrifugation, the top (T) fraction containing the liposome-bound proteins and bottom (B) fraction were collected and analyzed by SDS-PAGE. Proteins were stained with SYPRO orange. In F, the complete load (L) of each flotation is shown. (G) Principle of the generation of spin-labeled proteins for EPR analysis. Reaction of the (1-oxyl-2,2,5,5-tetramethylpyrrolidine-3-methyl) methanethiosulfonate spin label (MTSSL) with the sulfhydryl group of a cysteine side chain generates the spin label side chain R1. (H) Determination of the interactions of the spin labels attached to the Vps41 ALPS motif. EPR spectra (T = 293 K) of the doubly spin-labeled MBP-Vps41 fusion protein (336–402) with L366C and F373C mutations and single mutants. The spectrum of the labeled fusion protein (continuous line) is broadened compared with the sum of the spectra of the singly labeled samples (L366C or F373C; dashed line) caused by spin–spin interaction of the two R1 side chains, indicating close proximity of both nitroxides. For details see model in K and Radzwill et al. (2001). (I) Determination of the distance between two spin labels by low temperature EPR. Quantitative analysis of the dipolar broadening revealed in the low temperature EPR spectra (T = 160 K) of the double mutant (continuous line, compared with the sum of the spectra of the singly labeled samples, dashed line) yields a mean internitroxide distance of 1.1 \pm 0.2 nm. The dotted line shows the simulation of a corresponding dipolar broadened EPR spectrum. (J and K) Quantitation of the mean distance between the spin labels reveals that the segment can form an α helix. Interspin distance distribution determined from I (continuous line) superimposed to an internitroxide distance distribution are shown, which were calculated from a molecular dynamics simulation for 30 ns at 300 K of the α -helical peptide sequence 361–377 with the spin label side chains introduced at positions 366 and 373 (dotted line) as shown in K and for the stretched peptide conformation (dashed line) as obtained from a rotamer analysis (Jeschke and Polyhach, 2007). *r*, relative distance. P(*r*), probability to find the distance *r*. DIC, differential interference contrast.

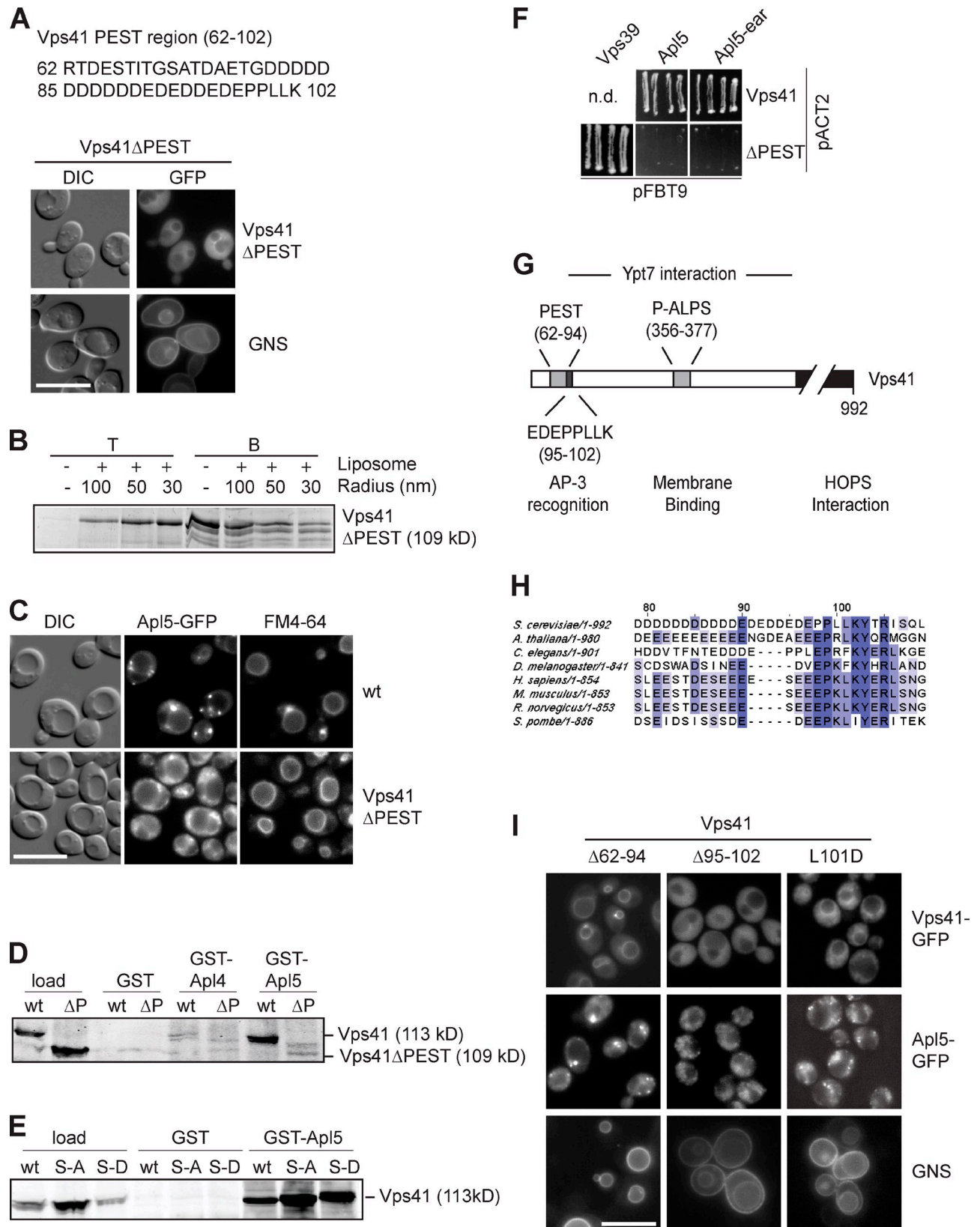


Figure 5. **PEST domain of Vps41 is necessary for interaction with Apl5.** (A) Effect of Vps41 PEST motif deletion on Vps41 localization and AP-3 sorting. Analysis of Vps41 Δ PEST-GFP and GNS localization in cells expressing the Δ PEST mutant was performed as in Fig. 4 E. (B) Interaction of purified Vps41 Δ PEST with membranes. The His-tagged fragment of Vps41(1–485) lacking the PEST domain was purified from *E. coli*, added to liposomes of different curvature, and subjected to flotation analysis as in Fig. 3 E. (C) Localization of Apl5-GFP in wt and Vps41 Δ PEST-expressing cells. Cells were stained with FM4-64 and analyzed by fluorescence microscopy. (D) Interaction of recombinant Apl5 with Vps41. Cell lysates were prepared from the indicated strains as described in Materials and methods and added to GSH-bound GST, GST-Apl5-ear (residues 803–932), and GST-Apl4-ear (residues 717–832), and

we sequentially truncated Vps41 and observed a pronounced defect in AP-3 cargo sorting if the first 102 residues of Vps41 were absent (unpublished data). This region of Vps41 harbors a PEST domain with a highly charged region from residues 62 to 102 (Fig. 5 A). A Vps41 mutant lacking this sequence, e.g., Vps41 Δ PEST, localized less efficiently to vacuoles (Fig. 5 A), though the protein was still assembled into the HOPS complex (Fig. S4 C) and interacted with liposomes in a curvature-dependent manner as before (Fig. 5 B). Importantly, the cells expressing this construct had an AP-3-sorting defect while maintaining normal vacuole morphology (Fig. 5 A) and protein sorting via endosomes (not depicted). The Vps41 mislocalization and AP-3-sorting defect could not be rescued by additional mutations in the ALPS motif (Fig. S4, A and E). Moreover, Apl5-GFP localization was strongly affected, resulting in multiple dispersed dots throughout the cell (Fig. 5 C). We then generated GST fusion proteins carrying the C-terminal domain of Apl4 or Apl5 and used them for pull-down assays together with yeast lysates expressing Vps41 wt or Vps41 Δ PEST. Vps41 specifically bound to GST-Apl5 but not Apl4 (Fig. 5 D). This binding was not affected by S-D or S-A mutations (Fig. 5 E), but it required the N-terminal PEST domain (Fig. 5 D). This interaction was confirmed by a yeast two-hybrid analysis (Fig. 5 F). In view of the charge density of the Vps41 PEST domain, the binding to Apl5 could be simply caused by nonspecific charge-charge interactions. However, a closer inspection of the PEST domain revealed that not only the negatively charged residues 62–94 but also residues 95–102 of Vps41 are highly conserved (Fig. 5, G and H; Lu et al., 2007). We therefore generated additional Vps41 truncations of the PEST subdomains, Vps41(Δ 62–94) and Vps41(Δ 95–102). Whereas the Vps41(Δ 62–94) mutant localized to vacuoles and was functional in the AP-3 pathway, the Vps41(Δ 95–102) mutant resulted in an AP-3-sorting defect and Apl5 mislocalization (Fig. 5 I). A point mutant within the second region, L101D, was defective in the AP-3 pathway, though it is localized to the vacuole (Fig. 5 I). We conclude that Vps41 recognizes the δ subunit of the AP-3 complex via a sequence with similarity to the dileucine-sorting motif of the AP-3 cargo.

Phosphorylation permits Vps41 to function in the AP-3 pathway

How does ALPS phosphorylation influence the function of Vps41 in the AP-3 pathway? The N-terminal region (residues 114–366) of Vps41 is predicted to form a β propeller (McMahon and Mills, 2004), and as a result, the Apl5-binding site (residues

95–102) and the ALPS motif (residues 356–376) might be close to each other in the folded protein. Thus, one possible scenario would be that the binding of the ALPS motif to the endosome membrane masks the Apl5-binding site, and Yck3 will only get access to the Vps41 at the vacuole because it is routed via the AP-3 pathway. The release and phosphorylation of the ALPS motif would make Vps41 available for interaction with AP-3 vesicles only at the vacuole. We tested this hypothesis with the liposome flotation assay.

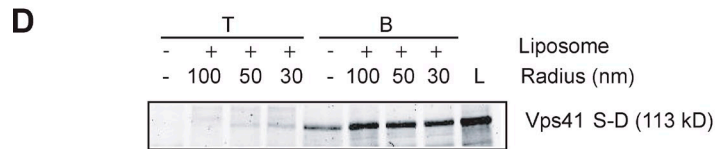
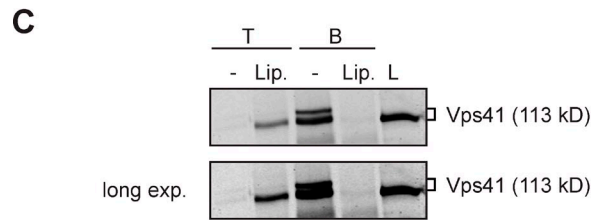
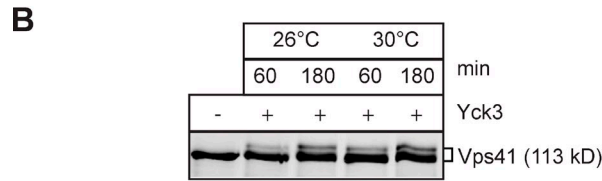
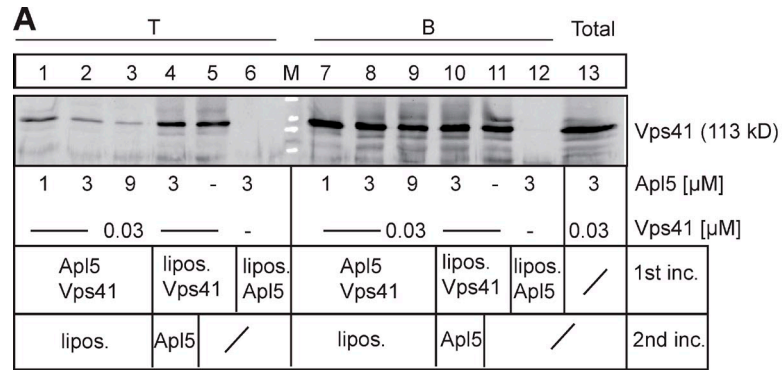
We first determined whether Vps41, once bound to liposomes, can still interact with Apl5. The former occurs at the late endosome, and the latter—Apl5 binding—occurs at the vacuole. In principle, one would expect a simple competition between liposomes and Apl5 for Vps41. When Vps41 was incubated first with liposomes, it was floating efficiently as before and not influenced by subsequent addition of Apl5 (Fig. 6 A, lanes 4 and 5). In contrast, preincubation of Vps41 with increasing amounts of Apl5 prevented the interaction of Vps41 with liposomes, as is evident from the poor recovery of Vps41 in the top fraction of the flotation assay (Figs. 6 A, lanes 1–3; and S3 C). The inhibitory effect of Apl5 in turn indicates that liposome-bound Vps41 cannot bind to Apl5. This observation is consistent with our hypothesis that membrane binding hides the Apl5-binding site of Vps41 on late endosomes.

Second, liposome-bound Vps41 should not be accessible to Yck3, and Yck3 should only phosphorylate nonmembrane-bound Vps41. Recombinant Yck3 was able to phosphorylate Vps41 in vitro, resulting in a similar size shift as reported previously (Fig. 6 B; LaGrassa and Ungermann, 2005; Brett and Merz, 2008; Brett et al., 2008; Hickey et al., 2009). However, preincubation of Vps41 with liposomes made it insensitive to Yck3 (Fig. 6 C), indicating that Yck3 cannot access the membrane-embedded helix of Vps41. Moreover, only the nonphosphorylated Vps41 floated with liposomes (Fig. 6 C), whereas the phosphomimetic mutant (S-D) remained unbound (Fig. 6 D). This observation confirmed the idea that Vps41 binds endosomal membranes via the ALPS motif. At the vacuoles, the N-terminal domain of Vps41 is released from the membrane because of changes in curvature or composition and only then can be phosphorylated by Yck3. Vps41 then binds Apl5 and, thus, recognizes AP-3 vesicles (Fig. 6 E).

Our model predicted that the *YCK3* deletion can be suppressed by mutants in the Vps41 ALPS motif. We therefore analyzed the GNS sorting in ALPS mutants combined with the *YCK3* deletion. Importantly, both Vps41 S-D and Vps41 Δ ALPS restored the AP-3 pathway regardless of the presence or absence

bound proteins were eluted by boiling in SDS sample buffer. Eluted proteins were analyzed by SDS-PAGE and Western blotting using anti-Vps41 antibodies. (E) Interaction of Vps41 S-A and S-D mutants with Apl5. Pull-down was conducted as in D using lysates obtained from strains expressing the indicated Vps41 variants. (F) Yeast two-hybrid analysis. *VPS39*, *APL5*, and *APL5*-ear (residues 803–932) domains were cloned in the pFBT9 vectors, whereas Vps41 and Vps41 Δ PEST were cloned in the pACT2 vector. Plasmids were cotransformed into the strains for yeast two-hybrid analysis and grown on double-dropout and quadruple-dropout plates. Only quadruple-dropout plates are shown. See Materials and methods for details. (G) Overview of the interaction sites within the N-terminal region of Vps41. The N-terminal half of the protein contains binding sites for Apl5 (PEST) and membrane (phosphorylated ALPS [P-ALPS]), whereas the C-terminal part is required for HOPS binding. (H) Sequence alignments of the Vps41 N-terminal sequence proximal to the PEST domain from different species using the ClustalW algorithm. Conserved residues are highlighted. Dark purple, highly conserved residues. Light purple, conserved residues. (I) Identification of the minimal domain in Vps41 required for AP-3 sorting. Vps41 truncations Δ 62–94 and Δ 95–102 and L101D mutant were analyzed by fluorescence microscopy to determine Vps41 distribution, Apl5-GFP localization, and GNS sorting. Note that none of the mutants disrupts vacuole morphology. DIC, differential interference contrast. n.d., not determined. Bars, 10 μ m.

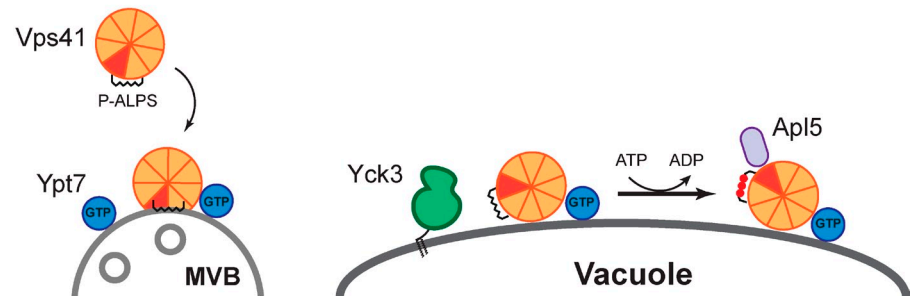
Figure 6. Counteraction of membrane binding and interaction with Apl5. (A) Apl5 binding to Vps41 inhibits binding to liposomes. Vps41 was preincubated for 5 min with increasing amounts of GST-Apl5-ear (lanes 1–3 and 7–9) and then incubated for 5 min with small liposomes (30 nm) at room temperature. As a comparison, Vps41 was preincubated with liposomes for 5 min, and Apl5 was then added (lanes 4 and 10). All samples were used for the flotation assay as described in Fig. 3 E and Materials and methods. As controls, Vps41 (lanes 5 and 11) or Apl5 (lanes 6 and 12) were incubated with liposomes. After centrifugation, top (T) and bottom (B) fractions were collected and TCA precipitated before analyzing proteins by Western blotting using anti-Vps41 antibodies. (B) Vps41 phosphorylation by Yck3. 0.28 μ M of full-length Vps41 was incubated at the indicated temperature and time periods with 12 μ M of recombinant Yck3, and phosphorylation was monitored by immunoblot analysis using anti-Vps41 antibodies. (C) Liposome binding abolishes Vps41 phosphorylation. Full-length Vps41 was incubated with small liposomes or buffer containing 1 mM Mg^{2+} -ATP for 5 min before adding Yck3 for 30 min at room temperature. Samples were then subjected to flotation in a sucrose gradient as in Fig. 3 E. The proteins in the top (T) and bottom (B) fractions were TCA precipitated and then analyzed by SDS-PAGE followed by SYPRO orange staining. The long exposure (exp.) confirms that no phosphorylated Vps41 is in the top fraction. L, load. Lip., liposome. (D) Flotation of phosphorylated Vps41. Liposome flotation was performed as in Fig. 3 E with the N-terminal domain of Vps41(1–484) carrying the S367, 368, 371, and 372D mutations (S-D). (E) Model of Vps41 and Apl5 interaction on endosomes and vacuoles. On endosomes, binding of Vps41 masks the Apl5-binding site, which becomes available on vacuoles. P-ALPS, phosphorylated ALPS.



E

High curvature
yck3 Δ

Low curvature
Yck3-mediated phosphorylation



of Yck3 (Fig. 7 A). This indicated that the loss of ALPS phosphorylation can be bypassed by lowering the ALPS affinity for membranes. Mutations of the ALPS motif can then facilitate proper Vps41 function in the AP-3 pathway.

We postulated that a relocalization of Yck3 to the late endosome should affect Vps41 localization and function by triggering premature ALPS phosphorylation, presumably before it even inserts into the membrane. To confine Yck3 function primarily to the late endosome, we fused the EEA1 FYVE domain to the C terminus of this kinase. The GFP-tagged Yck3-FYVE fusion protein accumulated in multiple dots proximal to the

vacuole, reminiscent of the late endosome (Fig. 7 B). Interestingly, Vps41 and Vps39 normally localized to the vacuoles (Figs. 7 C and S5), and these cells had a functional AP-3 pathway, unlike *yck3 Δ* cells (Fig. 7 D), suggesting that Yck3 could indeed activate Vps41 already at the late endosome. However, it was possible that the premature phosphorylation of Vps41 would weaken its binding to membranes. We therefore GFP-tagged Ypt7 in the Yck3-FYVE background to determine how tightly Vps41 was bound to membranes. Indeed, with GFP-tagged Ypt7, vacuoles started to lose their normal round structures (Fig. 7 E). These results confirmed that the endosome

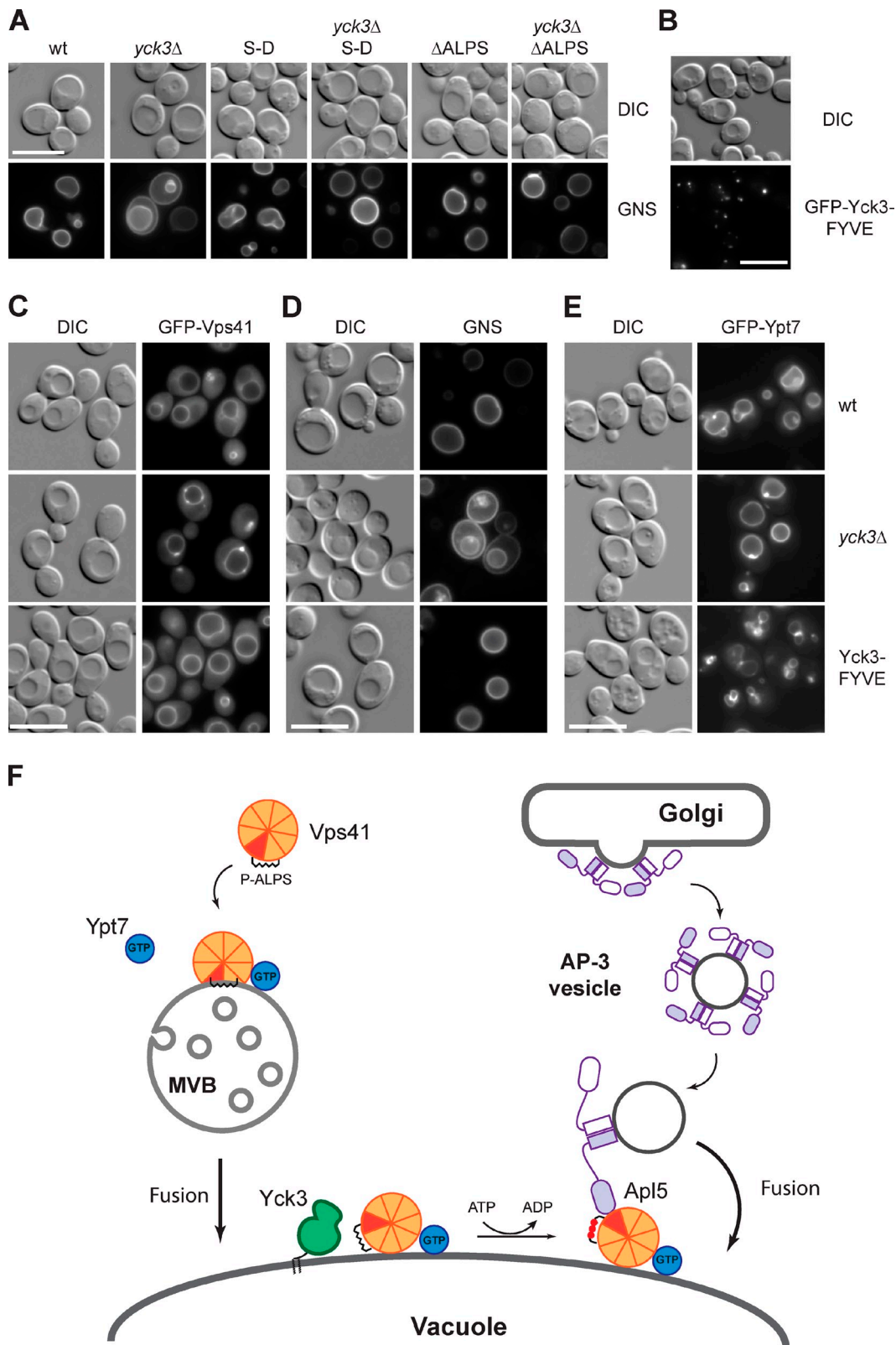


Figure 7. **Vps41 function in the AP-3 pathway is activated by Yck3.** (A) ALPS mutants can rescue AP-3 defects in *yck3Δ* cells. The AP-3 pathway was monitored after GNS sorting in the *yck3Δ* background expressing Vps41 S-D or Δ ALPS mutants. (B–E) Endosome targeting of Yck3 abolishes Vps41 localization at the late endosomes. (B) Endosome targeting of Yck3 kinase by a FYVE domain. GFP-tagged Yck3 containing the EEA1 FYVE domain at its C terminus was analyzed by fluorescence microscopy. Localization of GFP-tagged Vps41 (C), GNS (D), and GFP-Ypt7 (E) was visualized in wt, *yck3Δ*, and cells expressing Yck3 containing a FYVE domain. (F) Model of Vps41 switching to function in AP-3 vesicle fusion. The β propeller (orange) contains the Apl5-binding site (red), the ALPS motif (black helix), and the Ypt7-binding site. HOPS binding requires the C-terminal part (not depicted). The HOPS complex has been omitted for clarity here. On MVBs, the Apl5-binding site is masked and only becomes available once vacuolar Yck3 (green) phosphorylates the ALPS (indicated by red dots). At the vacuole, Ypt7 (blue) still binds Vps41/HOPS. Phosphorylation also allows Vps41 partitioning to the cytosol. DIC, differential interference contrast. P-ALPS, phosphorylated ALPS. Bars, 10 μ m.

targeting of Yck3 destabilized Vps41 at the late endosome and affected its functionality in endosome–vacuole fusion.

Collectively, our data reveal that Vps41 localization to MVBs is controlled by a dual targeting mechanism consisting of the Rab GTPase Ypt7 and a membrane contact site (ALPS). Association of Vps41 with endosomes masks an AP-3–binding site that is only exposed by Yck3-mediated phosphorylation at the vacuole.

Discussion

We report here on a novel mechanism that allows one tethering complex, depending on its localization, to operate in two different trafficking pathways (Fig. 7 F). Vps41 is part of the HOPS-tethering complex, which is present on both late endosomes and vacuoles. On late endosomes, Vps41 is dedicated to endosome–vacuole fusion and does not interact with AP-3 vesicles, whereas it becomes available for AP-3 vesicle fusion on vacuoles. Our data now explain the molecular basis of the localization-dependent fusion specificity.

Vps41 has at least four important binding sites that are critical for its function (Figs. 5 H and 7 F). Within its N-terminal β propeller, it binds Ypt7-GTP (Brett et al., 2008; Ostrowicz et al., 2010) and either the AP-3 δ subunit Apl5 or highly curved membranes via its ALPS motif. Binding to the remaining HOPS requires the C-terminal portion. On late endosomes, the binding of Vps41 to membranes via its ALPS motif masks the Apl5-binding site, thereby preventing fusion of AP-3 vesicles with the wrong target organelle (Fig. 7 F). This is important because the AP-3 pathway delivers the kinase Yck3 (Sun et al., 2004), which, if ending up at MVBs, would inactivate the ALPS membrane-binding motif in Vps41. Accordingly, mutations in the ALPS motif lead to an increase of cytosolic Vps41 and enhanced sensitivity to GFP tagging of the Rab Ypt7. Moreover, the syntaxin SNARE Vam3 arrives at the vacuole via the AP-3 pathway. If misrouted via the endosome, these endosomes will be identified as vacuoles and fuse prematurely (Darsow et al., 1998). Similarly, the R-SNARE Nyv1, which is dedicated to vacuole fusion, arrives exclusively via the AP-3 pathway (Reggiori et al., 2000; Wen et al., 2006). Once MVBs fuse with vacuoles, the change in membrane curvature and, presumably, also the membrane composition reduces the affinity of the ALPS motif for membranes. In addition, the phosphorylation of residues within the ALPS motif by Yck3 prevents the reinsertion into membrane of this α helix and, thus, exposes the Apl5-binding site of Vps41 to the cytosol. As a consequence, Vps41, and thus the HOPS complex, can interact with AP-3 vesicles and ensure their exclusive fusion with the vacuole-limiting membrane (Fig. 7 F). Importantly, the spatial separation of enzyme and substrate guarantees that Vps41 will recognize AP-3 vesicles only at the vacuole membrane while maintaining efficient targeting and functioning of Vps41 at MVBs.

Molecular function of the ALPS motif

The basic function of the ALPS motif is to sense membrane curvature and was first described in ArfGAP1, the GTPase-activating protein for Arf1 (Bigay et al., 2003). ArfGAP1 activity responds

to membrane curvature and couples the COPI vesicle biogenesis with coat disassembly. GMAP-210 constitutes another example of an ALPS-containing protein that uses an α helix to discriminate between transport vesicles and Golgi membranes (Drin et al., 2008). Modulation of the Vps41 ALPS motif can affect protein localization and function in vivo and change HOPS activity in vitro if small liposomes are used in the fusion assay (Hickey et al., 2009). Under these conditions, HOPS binding to Ypt7-GTP is still required (Cabrera et al., 2009).

We propose that the Vps41 ALPS motif supports its localization to endosomes, but we cannot exclude that it also recognizes high curvature domains at the vacuole. This would explain the resistance of *yck3 Δ* vacuoles to Rab GTPase inhibitors in vivo and in vitro (LaGrassa and Ungermann, 2005; Brett et al., 2008; Cabrera et al., 2009). In the absence of the Yck3 kinase, Vps41 ALPS will interact more efficiently with membranes and, as a result, stabilize Vps41 interaction with the Rab GTPase Ypt7, thus shielding it from inactivation by the GTPase-activating protein (Cabrera et al., 2009). The Ypt7-binding site is, just as the ALPS motif, part of the N-terminal domain (Ostrowicz et al., 2010) and required for HOPS targeting and function (Cabrera et al., 2009). Interestingly, isolated vacuoles from *yck3 Δ* cells contain more tightly bound Vps41 (LaGrassa and Ungermann, 2005; Brett et al., 2008), suggesting that the vacuole membrane maintains local curvature even after isolation. The sensitivity of vacuoles and cells to Ypt7 inhibitors upon changes in osmolarity (LaGrassa and Ungermann, 2005; Brett and Merz, 2008; Takeda et al., 2008) can then be explained by alterations in the Vps41–membrane interaction and the accessibility of the ALPS to the Yck3 kinase.

We propose that the Vps41 ALPS motif is a sensor of the membrane microenvironment, which is regulated by a casein kinase that permits functional switch and protein recycling. This motif intrinsically combines several advantages. It is a curvature sensor, not an inducer, and its membrane-sensing activity can be modulated by phosphorylation of its serine or threonine residues in the polar face. This can also be achieved if the kinase is rather nonspecific and ubiquitous, which shifts the level of regulation to the accessibility of the ALPS motif. We therefore term such a motif phospho-ALPS (P-ALPS; palps describes the sensory organs of insects). We suggest that yeast cells take advantage of the large size difference between MVBs and vacuoles for this additional level of regulation. It is likely that mammalian cells have evolved alternative regulatory loops to control the interaction of Rab7 and the HOPS complex.

The modulation of membrane sensors, as observed here for yeast Vps41, could be a common theme in membrane regulation in eukaryotic cells, and we expect that several of the identified ALPS motifs are targets for phosphorylation. Indeed, the ALPS motifs identified in the Golgi proteins ArfGAP1 (T215) and GMAP-210 (S22) could be targets of PKC and PKA, respectively (based on NetPhos 2.0), and phosphorylation of either protein might control Golgi morphology in mammalian cells.

Regulation of the AP-3 pathway

The AP-3 pathway is conserved across species, and Vps41 has been implicated in the trafficking of AP-3 vesicles in *Drosophila*

melanogaster and mammals (Warner et al., 1998; Rehling et al., 1999; Darsow et al., 2001; McVey Ward et al., 2001; Angers and Merz, 2009). In yeast and metazoans, AP-3 vesicles appear to fuse only with mature endosomes or lysosomes, bypassing MVBs (Dell'Angelica, 2009). Yeast utilizes the ALPS motif in Vps41 to target AP-3 vesicles exclusively to the vacuole, whereas such a motif is missing in metazoan Vps41 (Lu et al., 2007). This finding raises an intriguing question: Which mechanism allows the AP-3 pathway to bypass the immature endosomes in metazoan cells? It is possible that Vps41 is only recruited lately to maturing MVBs, and then the cargo proteins of the AP-3 vesicles are not sorted into MVBs or endosomes. Consistent with this idea, in yeast, both AP-3 cargoes Nyv1 and Vam3 are partially sorted into the vacuole lumen if they are diverted into the endocytic pathway (Reggiori et al., 2000).

According to our observations, fusion of the AP-3 vesicles with the yeast vacuole will differ in several aspects from fusion of late endosomes with vacuoles. Fusion of late endosomes with vacuoles will most likely mirror the requirements of vacuole–vacuole fusion (Ostrowicz et al., 2008). Indeed, Vps41 and Ypt7, components of the vacuole-tethering machinery, can be observed on late endosomes (Fig. 1 D; kleine Balderhaar et al., 2010), consistent with findings in mammalian cells (Chavrier et al., 1990). In addition, the Ypt7 guanine nucleotide exchange factor, the Mon1–Ccz1 complex, has been localized to late endosomes in yeast and metazoans (Nordmann et al., 2010; Poteryaev et al., 2010). Interestingly, the sorting of Vps41 to endosomes via a FYVE domain does not result in vacuole fragmentation, suggesting that Vps41 mainly arrives at the vacuole through the endosomes and not directly from the cytosol. Our data indicate that Vps41 is recruited to endosomes also if not assembled into the HOPS complex (Fig. 2), and HOPS could be assembled at the late endosome. However, we cannot exclude that HOPS is recruited as a complex to both vacuoles and late endosomes. Thus, the HOPS-mediated tethering, which may include SNARE binding (Stroupe et al., 2009), could then promote endosome–vacuole fusion. This symmetric tethering, in which the same constituents, HOPS and SNAREs, are found on both membranes, differs from the asymmetric tethering of AP-3 vesicles with vacuoles. Here, AP-3 vesicles are recognized by their coat via vacuole-localized Vps41, an event likely to precede HOPS- and SNARE-mediated fusion.

Our data then add Vps41 and Apl5 to the list of identified tether–coat interactions (Andag and Schmitt, 2003; Cai et al., 2007) and suggest a general mechanism of vesicle recognition (Angers and Merz, 2010). Interestingly, the AP-3–binding motif in Vps41 has some similarity to the AP-3–sorting motif in Pho8/ALP and Vam3 (Darsow et al., 1998), the SNARE that mediates fusion of AP-3 vesicles with the vacuole. Potentially, the binding of the Apl5 ear domain to Vam3 inactivates the SNARE on AP-3 vesicles until the vacuole-localized Vps41 releases Apl5 from Vam3 and makes it available for fusion of the AP-3 vesicle with the vacuole. Such a model is consistent with recent observations that indicate that the HOPS complex binds to Apl5 at the vacuole (Angers and Merz, 2009).

To summarize, we present a mechanism by which a tethering protein can fulfill its function in two distinct trafficking

pathways by masking one specialized binding site until the tethering protein is localized to the correct compartment. Similar mechanisms could explain targeting specificity of trafficking pathways in the endomembrane system, such as the tethering of Cvt vesicles or autophagosomes with the vacuole.

Materials and methods

Yeast strains and molecular biology

The yeast strains used in this study are summarized in Table S1. Yeast was grown at 30°C in rich medium (yeast peptone D-glucose [YPD]) except where indicated. Deletions and tagging of genes with GFP were performed using homologous recombination of PCR-amplified fragments (Puig et al., 1998; Janke et al., 2004). *VPS41* was expressed from a pRS406 under the *NOP1* promoter. Point mutations in *VPS41* were generated using a site-directed mutagenesis kit (QuickChange; Agilent Technologies). The vector pHis-Parallel coding Yck3 sequence (residues 2–516) was transformed into the BL21 (DE3) Rosetta *Escherichia coli* strain for protein expression (Hickey et al., 2009). Plasmids were provided by Christopher Hickey and Bill Wickner (Dartmouth Medical School, Hanover, NH). BL21 (DE3) Rosetta cells were grown to an OD₆₀₀ of ~0.6–0.8 before inducing protein expression with 0.5 mM IPTG overnight at 16°C. Protein purification was performed using the Ni–nitrilotriacetic acid resin (QIAGEN), and elution was performed with 300 mM imidazole. Buffer exchange to 20 mM Pipes/KOH, pH 6.8, and 200 mM sorbitol was performed with a PD10 column (GE Healthcare). Expression of MBP-Vps41 (residues 336–403) was induced with 0.5 mM IPTG overnight at 16°C, and the fusion protein was purified using amylose resin (New England Biolabs, Inc.).

Liposome preparation

Lipids were purchased from Avanti Polar Lipids, Inc., except for ergosterol (Sigma-Aldrich), phosphatidylinositol-3-phosphate, and PI-4,5-P₂ (Mobitech/Echelon). A lipid film containing 47% dioleoyl-phosphatidylcholine, 18% dioleoyl-phosphatidylethanolamine, 18% soy phosphatidylinositol, 4.4% dioleoyl-phosphatidylserine, 2% dioleoyl-phosphatidic acid, 1.6% cardiolipin, 8% ergosterol, 1% DAG, 1% phosphatidylinositol-3-phosphate, 1% PI-4,5-P₂, and 1% NBD-phosphatidylethanolamine (Zinser et al., 1993; Mima et al., 2008) was prepared by evaporation and resuspended in Hepes-KOAc (HK) buffer (50 mM Hepes/KOH, pH 7.2, and 120 mM KOAc). After five steps of thawing and freezing in liquid nitrogen, the 2-mM liposome suspension was extruded sequentially through polycarbonate filters with pore sizes of 400, 200, 100, 50, and 30 nm using a hand extruder (Avanti Polar Lipids, Inc.). The liposome radius was determined by dynamic light scattering in a DynaPro system (Wyatt Technology Corp.).

Flotation experiments

0.75 μM of proteins was mixed with 0.75 mM of liposomes in 150 μl HKM buffer (HK buffer with 1 mM MgCl₂) at room temperature for 5 min. 100 μl of a 75% sucrose solution in HKM buffer was added to adjust the sucrose concentration to 30%. The suspension was overlaid with two cushions (200 μl of a 25% sucrose solution in HKM and 50 μl HKM buffer). The sample was centrifuged at 220,000 g in a swing rotor (TLS 55; Beckman Coulter) for 1 h at 20°C. The bottom (250 μl), middle (150 μl), and top (50 μl) fractions were collected, and TCA-precipitated proteins were analyzed by SDS-PAGE using SYPRO orange (Invitrogen) staining or immunoblotting. The gels were visualized in a VersaDoc imaging system and quantified using Quantity One software (Bio-Rad Laboratories).

Yeast two-hybrid analysis

Yeast two-hybrid analysis was performed as previously described (Shorter et al., 1999). Combinations of pACT2– and pBTD9–yeast two-hybrid vectors carrying the DNA sequence of the indicated proteins were transformed into the yeast strain PJ69-4A and plated onto synthetic media lacking leucine and tryptophane (double dropout). Transformants were transferred first onto medium lacking leucine, tryptophane, histidine, and adenine (quadruple dropout) and afterward on double-dropout medium. For each combination of yeast two-hybrid–vector, four clones were analyzed.

Microscopy

Cells were grown to mid–logarithmic phase in YPD or synthetic complete medium lacking selected amino acids or nucleotides, harvested by centrifugation, washed once with synthetic complete medium supplemented with all amino acids, and visualized at room temperature. For FM4-64 (Invitrogen)

labeling of the vacuoles, cells were grown to an OD₆₀₀ of ~0.5 and incubated in YPD medium containing 30 μM FM4-64 for 30 min. After being washed with YPD medium, cells were incubated in the same medium without dye for 1 h. Cells were imaged using an epifluorescence microscope (DM5500 B; Leica) equipped with differential interference contrast optics, an HCX PL APO 100× 1.46 or 1.4–0.7 oil objective lens, a camera (SPOT Pursuit; Diagnostic Instruments, Inc.; or DFC 350 FX; Leica), and filter sets for GFP (excitation D480/30, emission D535/40, and beamsplitter 505 dichroic long pass), RFP (excitation 61000v2x, emission 61000v2m, and beamsplitter 61000v2bs), and FM4-64 (excitation D535/50×, emission E590LPv2, and beamsplitter 565 dichroic long pass; Chroma Technology Corp.). Images were captured using image acquisition and analysis software (Metamorph 7; Visitron Systems), and brightness and contrast were adjusted with ImageJ 1.42 (National Institutes of Health) and Photoshop CS3 (Adobe).

Electron microscopy analysis

Nanogold labeling and immunoelectron microscopy analyses were performed as previously described (Griffith et al., 2008; Cabrera et al., 2009; Griffith and Reggiori, 2009).

Cell lysis and membrane fractionation

To prepare lysates, yeast was grown in YPD to an OD₆₀₀ of ~1. Cells were harvested by centrifugation and treated with 10 mM DTT followed by an incubation with lyticase for 20 min at 30°C. Spheroplasts were then resuspended in lysis buffer (200 mM sorbitol, 50 mM KOAc, 20 mM Hepes-KOH, pH 6.8, protease inhibitor cocktail [0.1 μg/ml leupeptin, 1 mM α-phenanthroline, 0.5 μg/ml pepstatin A, and 0.1 mM pefablock], 1 mM PMSF, and 1 mM DTT) containing 2 μg/ml DEAE-dextran and incubated on ice for 5 min, followed by a 2-min incubation at 30°C. Lysates were centrifuged at 300 g for 3 min at 4°C, and the resulting supernatant was then sedimented at 20,000 g for 15 min to obtain P20 (pellet) and S20 (supernatant) fractions. The S20 fraction was then centrifuged at 100,000 g for 1 h to generate P100 (pellet) and S100 (supernatant) fractions. TCA-precipitated supernatants and pellets were resuspended in SDS sample buffer, loaded onto SDS-PAGE gels, and subjected to Western blot analyses.

Vps41 phosphorylation assay

P20 membrane fractions were incubated for 45 min at 26°C in phosphatidylserine buffer supplemented with salts (0.5 mM MgCl₂, 0.5 mM MnCl₂, and 125 mM KCl; Mayer et al., 1996) and 10 μM coenzyme A, with or without an ATP-regenerating system (0.5 mM ATP, 40 mM creatine phosphate, and 0.1 mg/ml creatine kinase). Membranes were reisolated by centrifugation at 20,000 g for 10 min at 4°C, and pellets were resuspended in SDS sample buffer. Vps41 mobility shift was analyzed by Western blotting using an anti-Vps41 antibody.

Immunoprecipitation

1 liter of culture was grown at 30°C to an OD₆₀₀ of ~4, and cells were harvested by centrifugation. Cells were then lysed in the following buffer: 50 mM Hepes/KOH, pH 7.4, 150 mM NaCl, 0.15% NP-40 (Igepal CA-630; Sigma-Aldrich), 1.5 mM MgCl₂, fungi yeast protease inhibitor mix (Serva), 0.5 mM PMSF, and 1 mM DTT. Cell lysates were then centrifuged at 100,000 g for 1.5 h, and supernatants were incubated with anti-GFP antibodies coupled to protein A-Sepharose (Ungermann et al., 1998) for 1 h at 4°C. Beads were isolated by centrifugation at 2,000 g for 5 min at 4°C and washed with 20 ml lysis buffer supplemented with 0.5 mM DTT. Bound proteins were eluted by incubation with 0.1 M glycine, pH 2.5, TCA precipitated, and subjected to immunoblotting.

GST pull-down experiments

The GST pull-down experiments were performed as previously described (Darsow et al., 2001). For pull-downs, 100 OD₆₀₀ cell equivalents were lysed in buffer containing 20 mM Hepes, pH 6.8, 50 mM KOAc, fungi yeast protease inhibitor mix, 1 mM PMSF, and 1 mM DTT and centrifuged at 3,000 g for 3 min at 4°C; the supernatant was adjusted to 1% Triton X-100 and incubated for 10 min at 4°C. The lysate was then centrifuged at 13,000 g for 10 min at 4°C, and the supernatant was incubated for 1 h at 4°C with GST, GST-Apl5-ear, or GST-Apl4-ear bound to glutathione Sepharose. Washing steps were performed as described in the previous paragraph. The bound material was eluted by incubation of the Sepharose with SDS sample buffer and incubation for 5 min at 95°C.

Online supplemental material

Fig. S1 shows sorting of ALP and Nvy1 by the AP-3 pathway. Fig. S2 shows that endosomal targeting of Vps39 is independent of the AP-3

pathway. Fig. S3 shows flotation assay with Vps41. Fig. S4 shows the combination of the ALPS and PEST mutants in Vps41. Fig. S5 shows localization of GFP-Vps39. Table S1 shows yeast strains used in this study. Online supplemental material is available at <http://www.jcb.org/cgi/content/full/jcb.201004092/DC1>.

We thank Bruno Antony for valuable advice; Christopher Hickey, Bill Wickner, and Chris Burd (University of Pennsylvania, Philadelphia, PA) for plasmids; and Markus Abeln, Arun Thomas John Peter, Jens Lachmann, Clemens Ostrowicz, and Jacob Piehler for support and discussions.

This work was supported by the Sonderforschungsbereich 431, the Hans-Mühlenhoff Foundation (grant to C. Ungermann), the Netherlands Organization for Health Research and Development (grant ZonMW-VIDI-917.76.329), and the Utrecht University (High Potential grant to F. Reggiori).

Submitted: 19 April 2010

Accepted: 14 October 2010

References

- Anand, V.C., L. Daboussi, T.C. Lorenz, and G.S. Payne. 2009. Genome-wide analysis of AP-3-dependent protein transport in yeast. *Mol. Biol. Cell.* 20:1592–1604. doi:10.1091/mbc.E08-08-0819
- Andag, U., and H.D. Schmitt. 2003. Dsl1p, an essential component of the Golgi-endoplasmic reticulum retrieval system in yeast, uses the same sequence motif to interact with different subunits of the COPI vesicle coat. *J. Biol. Chem.* 278:51722–51734. doi:10.1074/jbc.M308740200
- Angers, C.G., and A.J. Merz. 2009. HOPS interacts with Apl5 at the vacuole membrane and is required for consumption of AP-3 transport vesicles. *Mol. Biol. Cell.* 20:4563–4574. doi:10.1091/mbc.E09-04-0272
- Angers, C.G., and A.J. Merz. 2010. New links between vesicle coats and Rab-mediated vesicle targeting. *Semin. Cell Dev. Biol.* doi:10.1016/j.semcdb.2010.07.003
- Bigay, J., P. Gounon, S. Robineau, and B. Antony. 2003. Lipid packing sensed by ArfGAP1 couples COPI coat disassembly to membrane bilayer curvature. *Nature.* 426:563–566. doi:10.1038/nature02108
- Bigay, J., J.F. Casella, G. Drin, B. Mesmin, and B. Antony. 2005. ArfGAP1 responds to membrane curvature through the folding of a lipid packing sensor motif. *EMBO J.* 24:2244–2253. doi:10.1038/sj.emboj.7600714
- Brett, C.L., and A.J. Merz. 2008. Osmotic regulation of Rab-mediated organelle docking. *Curr. Biol.* 18:1072–1077. doi:10.1016/j.cub.2008.06.050
- Brett, C.L., R.L. Plemel, B.T. Lobinger, M. Vignali, S. Fields, and A.J. Merz. 2008. Efficient termination of vacuolar Rab GTPase signaling requires coordinated action by a GAP and a protein kinase. *J. Cell Biol.* 182:1141–1151. doi:10.1083/jcb.200801001
- Cabrera, M., C.W. Ostrowicz, M. Mari, T.J. LaGrassa, F. Reggiori, and C. Ungermann. 2009. Vps41 phosphorylation and the Rab Ypt7 control the targeting of the HOPS complex to endosome-vacuole fusion sites. *Mol. Biol. Cell.* 20:1937–1948. doi:10.1091/mbc.E08-09-0943
- Cai, H., S. Yu, S. Menon, Y. Cai, D. Lazarova, C. Fu, K. Reinisch, J.C. Hay, and S. Ferro-Novick. 2007. TRAPPI tethers COPII vesicles by binding the coat subunit Sec23. *Nature.* 445:941–944. doi:10.1038/nature05527
- Chavrier, P., R.G. Parton, H.P. Hauri, K. Simons, and M. Zerial. 1990. Localization of low molecular weight GTP binding proteins to exocytic and endocytic compartments. *Cell.* 62:317–329. doi:10.1016/0092-8674(90)90369-P
- Conibear, E., J.N. Cleck, and T.H. Stevens. 2003. Vps51p mediates the association of the GARP (Vps52/53/54) complex with the late Golgi t-SNARE Tlg1p. *Mol. Biol. Cell.* 14:1610–1623. doi:10.1091/mbc.E02-10-0654
- Cowles, C.R., G. Odorizzi, G.S. Payne, and S.D. Emr. 1997. The AP-3 adaptor complex is essential for cargo-selective transport to the yeast vacuole. *Cell.* 91:109–118. doi:10.1016/S0092-8674(01)80013-1
- Darsow, T., C.G. Burd, and S.D. Emr. 1998. Acidic di-leucine motif essential for AP-3-dependent sorting and restriction of the functional specificity of the Vam3p vacuolar t-SNARE. *J. Cell Biol.* 142:913–922. doi:10.1083/jcb.142.4.913
- Darsow, T., D.J. Katzmman, C.R. Cowles, and S.D. Emr. 2001. Vps41p function in the alkaline phosphatase pathway requires homo-oligomerization and interaction with AP-3 through two distinct domains. *Mol. Biol. Cell.* 12:37–51.
- Dell'Angelica, E.C. 2009. AP-3-dependent trafficking and disease: the first decade. *Curr. Opin. Cell Biol.* 21:552–559. doi:10.1016/j.cob.2009.04.014
- Drin, G., J.F. Casella, R. Gautier, T. Boehmer, T.U. Schwartz, and B. Antony. 2007. A general amphipathic alpha-helical motif for sensing membrane curvature. *Nat. Struct. Mol. Biol.* 14:138–146. doi:10.1038/nsmb1194

- Drin, G., V. Morello, J.F. Casella, P. Gounon, and B. Antonny. 2008. Asymmetric tethering of flat and curved lipid membranes by a golgin. *Science*. 320:670–673. doi:10.1126/science.1155821
- Gautier, R., D. Douguet, B. Antonny, and G. Drin. 2008. HELIQUEST: a web server to screen sequences with specific alpha-helical properties. *Bioinformatics*. 24:2101–2102. doi:10.1093/bioinformatics/btn392
- Griffith, J., and F. Reggiori. 2009. Ultrastructural analysis of nanogold-labeled endocytic compartments of yeast *Saccharomyces cerevisiae* using a cryosectioning procedure. *J. Histochem. Cytochem.* 57:801–809. doi:10.1369/jhc.2009.952952
- Griffith, J., M. Mari, A. De Mazière, and F. Reggiori. 2008. A cryosectioning procedure for the ultrastructural analysis and the immunogold labelling of yeast *Saccharomyces cerevisiae*. *Traffic*. 9:1060–1072. doi:10.1111/j.1600-0854.2008.00753.x
- Haas, A. 1995. A quantitative assay to measure homotypic vacuole fusion *in vitro*. *Methods Cell Sci.* 17:283–294. doi:10.1007/BF00986234
- Hickey, C.M., C. Stroupe, and W. Wickner. 2009. The major role of the Rab Ypt7p in vacuole fusion is supporting HOPS membrane association. *J. Biol. Chem.* 284:16118–16125. doi:10.1074/jbc.M109.000737
- Janke, C., M.M. Magiera, N. Rathfelder, C. Taxis, S. Reber, H. Maekawa, A. Moreno-Borchart, G. Doenges, E. Schwob, E. Schiebel, and M. Knop. 2004. A versatile toolbox for PCR-based tagging of yeast genes: new fluorescent proteins, more markers and promoter substitution cassettes. *Yeast*. 21:947–962. doi:10.1002/yea.1142
- Jeschke, G., and Y. Polyhach. 2007. Distance measurements on spin-labelled biomacromolecules by pulsed electron paramagnetic resonance. *Phys. Chem. Chem. Phys.* 9:1895–1910. doi:10.1039/b614920k
- kleine Balderhaar, H.J., H. Arlt, C.W. Ostrowicz, C. Bröcker, F. Sündermann, R. Brandt, M. Babst, and C. Ungermann. 2010. The Rab-GTPase Ypt7 is linked to retromer-mediated receptor recycling and fusion at the yeast late endosome. *J. Cell Sci.* In press.
- LaGrassa, T.J., and C. Ungermann. 2005. The vacuolar kinase Yck3 maintains organelle fragmentation by regulating the HOPS tethering complex. *J. Cell Biol.* 168:401–414. doi:10.1083/jcb.200407141
- Lu, S., T. Suzuki, N. Iizuka, S. Ohshima, Y. Yabu, M. Suzuki, L. Wen, and N. Ohta. 2007. *Trypanosoma brucei* vacuolar protein sorting 41 (VPS41) is required for intracellular iron utilization and maintenance of normal cellular morphology. *Parasitology*. 134:1639–1647.
- Mayer, A., W. Wickner, and A. Haas. 1996. Sec18p (NSF)-driven release of Sec17p (alpha-SNAP) can precede docking and fusion of yeast vacuoles. *Cell*. 85:83–94. doi:10.1016/S0092-8674(00)81084-3
- McMahon, H.T., and I.G. Mills. 2004. COP and clathrin-coated vesicle budding: different pathways, common approaches. *Curr. Opin. Cell Biol.* 16:379–391. doi:10.1016/j.ccb.2004.06.009
- McVey Ward, D., D. Radisky, M.A. Scullion, M.S. Tuttle, M. Vaughn, and J. Kaplan. 2001. hVPS41 is expressed in multiple isoforms and can associate with vesicles through a RING-H2 finger motif. *Exp. Cell Res.* 267:126–134. doi:10.1006/excr.2001.5244
- Mima, J., C.M. Hickey, H. Xu, Y. Jun, and W. Wickner. 2008. Reconstituted membrane fusion requires regulatory lipids, SNAREs and synergistic SNARE chaperones. *EMBO J.* 27:2031–2042. doi:10.1038/emboj.2008.139
- Nordmann, M., M. Cabrera, A. Perz, C. Bröcker, C.W. Ostrowicz, S. Engelbrecht-Vandré, and C. Ungermann. 2010. The Mon1-Ccz1 complex is the GEF of the late endosomal Rab7 homolog Ypt7. *Curr. Biol.* 20:1654–1659. doi:10.1016/j.cub.2010.08.002
- Ostrowicz, C.W., C.T. Meiringer, and C. Ungermann. 2008. Yeast vacuole fusion: a model system for eukaryotic endomembrane dynamics. *Autophagy*. 4:5–19.
- Ostrowicz, C.W., C. Bröcker, F. Ahnert, M. Nordmann, J. Lachmann, K. Peplowska, A. Perz, K. Auffarth, S. Engelbrecht-Vandré, and C. Ungermann. 2010. Defined subunit arrangement and Rab interactions are required for functionality of the HOPS tethering complex. *Traffic*. 11:1334–1346.
- Peplowska, K., D.F. Markgraf, C.W. Ostrowicz, G. Bange, and C. Ungermann. 2007. The CORVET tethering complex interacts with the yeast Rab5 homolog Vps21 and is involved in endo-lysosomal biogenesis. *Dev. Cell*. 12:739–750. doi:10.1016/j.devcel.2007.03.006
- Poteryaev, D., S. Datta, K. Ackema, M. Zerial, and A. Spang. 2010. Identification of the switch in early-to-late endosome transition. *Cell*. 141:497–508. doi:10.1016/j.cell.2010.03.011
- Puig, O., B. Rutz, B.G. Luukkonen, S. Kandels-Lewis, E. Bragado-Nilsson, and B. Séraphin. 1998. New constructs and strategies for efficient PCR-based gene manipulations in yeast. *Yeast*. 14:1139–1146. doi:10.1002/(SICI)1097-0061(19980915)14:12<1139::AID-YEA306>3.0.CO;2-B
- Radzwill, N., K. Gerwert, and H.-J. Steinhoff. 2001. Time-resolved detection of transient movement of helices F and G in doubly spin-labeled bacteriorhodopsin. *Biophys. J.* 80:2856–2866. doi:10.1016/S0006-3495(01)76252-2
- Reggiori, F., M.W. Black, and H.R. Pelham. 2000. Polar transmembrane domains target proteins to the interior of the yeast vacuole. *Mol. Biol. Cell*. 11:3737–3749.
- Rehling, P., T. Darsow, D.J. Katzmann, and S.D. Emr. 1999. Formation of AP-3 transport intermediates requires Vps41 function. *Nat. Cell Biol.* 1:346–353. doi:10.1038/14037
- Seals, D.F., G. Eitzen, N. Margolis, W.T. Wickner, and A. Price. 2000. A Ypt/Rab effector complex containing the Sec1 homolog Vps33p is required for homotypic vacuole fusion. *Proc. Natl. Acad. Sci. USA*. 97:9402–9407. doi:10.1073/pnas.97.17.9402
- Shorter, J., R. Watson, M.E. Giannakou, M. Clarke, G. Warren, and F.A. Barr. 1999. GRASP55, a second mammalian GRASP protein involved in the stacking of Golgi cisternae in a cell-free system. *EMBO J.* 18:4949–4960. doi:10.1093/emboj/18.18.4949
- Stenmark, H., R. Aasland, B.H. Toh, and A. D'Arrigo. 1996. Endosomal localization of the autoantigen EEA1 is mediated by a zinc-binding FYVE finger. *J. Biol. Chem.* 271:24048–24054. doi:10.1074/jbc.271.39.24048
- Stroupe, C., C.M. Hickey, J. Mima, A.S. Burfeind, and W. Wickner. 2009. Minimal membrane docking requirements revealed by reconstitution of Rab GTPase-dependent membrane fusion from purified components. *Proc. Natl. Acad. Sci. USA*. 106:17626–17633. doi:10.1073/pnas.0903801106
- Sun, B., L. Chen, W. Cao, A.F. Roth, and N.G. Davis. 2004. The yeast casein kinase Yck3p is palmitoylated, then sorted to the vacuolar membrane with AP-3-dependent recognition of a YXXPhi adaptin sorting signal. *Mol. Biol. Cell*. 15:1397–1406. doi:10.1091/mbc.E03-09-0682
- Takeda, K., M. Cabrera, J. Rohde, D. Bausch, O.N. Jensen, and C. Ungermann. 2008. The vacuolar V1/V0-ATPase is involved in the release of the HOPS subunit Vps41 from vacuoles, vacuole fragmentation and fusion. *FEBS Lett.* 582:1558–1563. doi:10.1016/j.febslet.2008.03.055
- TerBush, D.R., T. Maurice, D. Roth, and P. Novick. 1996. The Exocyst is a multi-protein complex required for exocytosis in *Saccharomyces cerevisiae*. *EMBO J.* 15:6483–6494.
- Ungar, D., T. Oka, E.E. Brittle, E. Vasile, V.V. Lupashin, J.E. Chatterton, J.E. Heuser, M. Krieger, and M.G. Waters. 2002. Characterization of a mammalian Golgi-localized protein complex, COG, that is required for normal Golgi morphology and function. *J. Cell Biol.* 157:405–415. doi:10.1083/jcb.200202016
- Ungermann, C., B.J. Nichols, H.R. Pelham, and W. Wickner. 1998. A vacuolar v-t-SNARE complex, the predominant form *in vivo* and on isolated vacuoles, is disassembled and activated for docking and fusion. *J. Cell Biol.* 140:61–69. doi:10.1083/jcb.140.1.61
- Warner, T.S., D.A. Sinclair, K.A. Fitzpatrick, M. Singh, R.H. Devlin, and B.M. Honda. 1998. The light gene of *Drosophila melanogaster* encodes a homologue of VPS41, a yeast gene involved in cellular-protein trafficking. *Genome*. 41:236–243. doi:10.1139/gen-41-2-236
- Wen, W., L. Chen, H. Wu, X. Sun, M. Zhang, and D.K. Banfield. 2006. Identification of the yeast R-SNARE Nvy1p as a novel longin domain-containing protein. *Mol. Biol. Cell*. 17:4282–4299. doi:10.1091/mbc.E06-02-0128
- Zinser, E., F. Paltauf, and G. Daum. 1993. Sterol composition of yeast organelle membranes and subcellular distribution of enzymes involved in sterol metabolism. *J. Bacteriol.* 175:2853–2858.